

Turbulent Mixed Flow of Free and Forced Convection Between Vertical Parallel Plates

Cha'o-Kung Chen,* Chen-Ping Chiu,* and Shun-Ching Lee†
National Cheng-Kung University, Tainan, Taiwan, Republic of China

In predicting the fully developed turbulent mixed flow of forced and natural convection, the one-equation model of turbulence for low Reynolds number flows is adopted. Finite-element solutions are carried out in the upward turbulent flow between vertical parallel plates at different wall temperatures. In this condition, the aiding and opposing flows arise simultaneously on the heated and cooled sides, respectively, and a fully developed condition is established. The solutions with and without the effect of buoyancy force are predicted and the comparisons are discussed. In these two situations, the mean velocity and temperature profiles, the locations of the maximum velocity, eddy diffusivities of momentum, Nusselt number, friction factor, and turbulence kinetic energy are presented. The substantial effects of the buoyancy force are also confirmed.

Nomenclature

| | | | |
|---------------|--|---------------|---|
| \tilde{A} | = global coefficient matrix | q^+ | = dimensionless heat flux = $ q /\rho c_p u^*(T_H - T_c)$ |
| a | = thermal diffusivity | Re | = Reynolds number = $2\langle u \rangle b/\nu$ |
| a_{ij} | = element of global coefficient matrix | Re_T | = local turbulent Reynolds number |
| a_T | = eddy diffusivity for heat | Re_T^+ | = dimensionless local turbulent Reynolds number |
| \tilde{B} | = global source vector | T | = temperature |
| b | = distance between parallel plates | T_c^+ | = dimensionless temperature normalized by the cooled-wall parameter = $(T - T_c)\rho c_p u^*/ q $ |
| b_j | = element of global source vector | T_H^+ | = dimensionless temperature normalized by the heated-wall parameter = $(T_H - T)\rho c_p u_H^*/ q $ |
| b^+ | = dimensionless distance between parallel plates = bu^*/ν | u | = time-averaged velocity in the x direction |
| c_p | = specific heat at constant pressure | u^+ | = dimensionless velocity = u/u^* |
| f_c | = friction factor = $2 \tau_c /\rho \langle u \rangle_c^2$ | u^* | = friction velocity = $\sqrt{ \tau_c /\rho}$ |
| f_H | = friction factor = $2 \tau_H /\rho \langle u \rangle_H^2$ | v | = velocity in y direction |
| G^+ | = buoyancy parameter = $g\beta(T_H - T_c)\nu/u^*3$ | x | = coordinate in the flow direction |
| Gr | = Grashof number based on temperature difference = $8g\beta(T_H - T_c)b^3/\nu^2$ | x^+ | = dimensionless coordinate in the flow direction = xu^*/ν |
| g | = gravitational acceleration | y | = distance from the cooled wall |
| K | = turbulence kinetic energy | y^+ | = dimensionless distance from the cooled wall = yu^*/ν |
| K^+ | = dimensionless turbulence kinetic energy = K/u^*2 | z | = correction factor defined by Eq. (40) |
| k | = von Karman constant | β | = thermal expansion coefficient |
| ℓ | = element length | δ | = distance from the cooled wall to the maximum velocity location |
| ℓ_{1D} | = mixing length in dissipation | δ^+ | = dimensionless distance = $\delta u^*/\nu$ |
| ℓ_{1D}^+ | = dimensionless mixing length in dissipation = $\ell_{1D}u^*/\nu$ | ε | = turbulent dissipation |
| ℓ_{1v} | = mixing length in diffusivity | θ | = dimensionless temperature = $(T - T_c)/(T_H - T_c)$ |
| ℓ_{1v}^+ | = dimensionless mixing length in diffusivity = $\ell_{1v}u^*/\nu$ | λ | = thermal conductivity |
| N_i | = shape function | ν | = kinematic viscosity |
| Nu_c | = Nusselt number = $4 q \delta/(\langle T \rangle_c - T_c)/\lambda$ | ν_T | = eddy diffusivity for momentum |
| Nu_H | = Nusselt number = $4 q (b - \delta)/(T_H - \langle T \rangle_H)/\lambda$ | ν_T^+ | = dimensionless eddy diffusivity for momentum = ν_T/ν |
| \tilde{P} | = turbulence production | ρ | = density |
| P_u | = viscous production | σ_T | = turbulent Prandtl number |
| P_0 | = buoyancy production | τ | = shear stress |
| Pr | = Prandtl number | | |
| p | = real pressure | | |
| p_s | = static pressure | | |
| p^+ | = dimensionless pressure = $\langle p \rangle/\rho u^*2$ | | |
| q | = heat flux | | |

Subscripts

| | |
|---------------------|---|
| c | = at the cooled wall |
| H | = at the heated wall |
| m | = momentum |
| o | = forced convection |
| $\langle \rangle$ | = averaged over the cross section, $0 \leq y \leq b$ |
| $\langle \rangle_c$ | = averaged over the cooled side, $0 \leq y \leq \delta$ |
| $\langle \rangle_H$ | = averaged over the heated side, $\delta \leq y \leq b$ |

Superscript

| | |
|-----|---------------------------------|
| $+$ | = normalized by wall parameters |
|-----|---------------------------------|

Received March 7, 1988; revision received Oct. 15, 1988. Copyright © 1989 American Institute of Aeronautics and Astronautics, Inc. All rights reserved.

*Professor, Department of Mechanical Engineering.

†Graduate Student, Department of Mechanical Engineering.

Introduction

COMBINED forced and natural convection heat transfer between two vertical parallel plates continues to be an important problem because of its fundamental nature as well as its many related engineering applications. In situations where a great temperature difference in the forced flowfield is present, the buoyancy force is generated by the density difference. The influence of buoyancy force on the turbulent transport phenomena of heat and momentum must be considered.

The mixed forced and natural convection between the two vertical parallel plates may be divided into the following two kinds of flows. "Aiding" flow refers to the situation in which the buoyancy force is in the same direction as the forced flow, and "opposing" flow refers to the opposite situation. The natures of these two kinds of flows turn out to be intrinsically different, especially in the distortion pattern of shear-stress distributions, because of the buoyancy force near the wall. Brown and Gauvin^{1,2} investigated the influence of buoyancy force on the heat-transfer rates and temperature fluctuations in aiding and opposing flows in a vertical heated tube. Buhr et al.³ studied the temperature profiles in liquid metals and the effect of superimposed free convection in turbulent flow. Hall and Price⁴ presented the solution of combined forced and free convection from a vertical heated plate to air. Kenning et al.⁵ investigated the local reduction in heat transfer resulting from the effects of buoyancy force in upward turbulent flow. Tanaka et al.⁶ presented the effects of buoyancy force and acceleration owing to thermal expansion on forced turbulent convection in vertical circular tubes. Generally, the preceding results indicated that, in the situation of aiding flow, the temperature distribution along the wall sometimes showed a local temperature rise because of the local impairment of heat transfer. However, for opposing flow, heat transfer was promoted and was better than the aiding flow at the same heat flux. In those flow configurations, however, it is difficult to clarify the effect of the buoyancy force on the turbulent transport phenomena since the flows are developing and are not in a fully developed condition.

Some previous mixed convection analytical approaches assumed that the expressions for the distribution of eddy diffusivities in the forced convection can be applied to mixed convection by taking into account the temperature dependence of fluid properties. But Khosla et al.⁷ showed that the eddy diffusivity models for the forced convection were found to be inadequate and the buoyancy force had substantial influence on the turbulent transport process. Nakajima et al.⁸ suggested that the mixing-length model is useful in turbulent flow, and the buoyancy effect should be considered together with the viscous effect in mixed convection flow at low Reynolds numbers. In order to predict the buoyancy effect on the turbulent transport process in mixed convection, Nakajima et al.⁸ extended the damping-factor model given by van Driest.⁹ But the results of the preceding model can be obtained only for the situation of low Grashof numbers. Tanaka et al.¹⁰ adopted a two-equation model and obtained results for the situation of high Grashof numbers by using the ϵ equation to calculate the mixing lengths. But, a zero temperature gradient in the direction of gravity was adopted for these solutions and the effect of buoyancy was neglected. Townsend¹¹ indicated that the buoyancy production should exist because of near isotropy in the fully turbulent region.

The current study attempts to examine the influence of the buoyancy force on transfer of heat and momentum in the turbulent mixed convection.

Analysis

Governing Equations

The fully developed combined flow between vertical plates maintained at different temperatures is shown in Fig. 1. The fluid is flowing upward and the Boussinesq approximation is

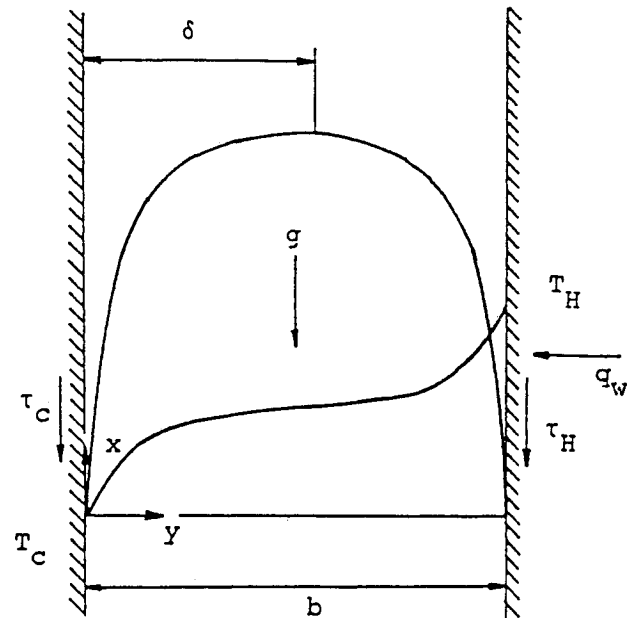


Fig. 1 Schematic phenomena of flow and heat transfer with isothermal walls at unequal temperatures.

used. The momentum and energy equations can be written as follows:

$$\frac{d}{dy} \left[(v + v_T) \frac{du}{dy} \right] - \frac{dp}{p dx} + \beta g (T - T_c) = 0 \quad (1)$$

$$\frac{d}{dy} \left[(a + a_T) \frac{dT}{dy} \right] = 0 \quad (2)$$

where T_c is the cooled wall temperature and $dp/dx = (dp_s/dx) + \rho g$, where p_s is the static pressure. The eddy diffusivities v_T and a_T for momentum and heat transfer, respectively, appearing in Eqs. (1) and (2) are given as

$$v_T = \ell_{1v} K^{1/2} \quad (3)$$

where $\ell_{1v} = C_D^{1/4} k_m y [1 - \exp(-0.016 R_T)]$, with $C_D = 0.09$ and

$$a_T = \frac{v_T}{\sigma_T} \quad (4)$$

The turbulent Prandtl number σ_T is assumed to be constant with the value of 0.85 according to the suggestion by Kader and Yaglom.¹² The fully developed turbulent kinetic energy equation is modeled phenomenologically by Ng and Spalding¹³ as

$$\frac{d}{dy} \left[(v + v_T) \frac{dK}{dy} \right] + \tilde{P} - \epsilon = 0 \quad (5)$$

In the current case of fully developed flow, $dT/dx = 0$. Based on the argument of near isotropy in the fully turbulent region, $u'T'$ is approximately equal to $v'T'$. Also, \tilde{P} should be constructed of viscous and buoyancy productions, i.e., $\tilde{P} = P_u + P_\theta$. The viscous production can be expressed by turbulent stress associated with the deformation of the mean flow as

$$P_u = v_T \left(\frac{du}{dy} \right)^2 \quad (6)$$

Similarly, the buoyancy production can be expressed by turbulent heat flux introduced by Townsend¹¹ as

$$P_\theta = a_T \beta g \left| \frac{dT}{dy} \right| \quad (7)$$

The viscous dissipation of turbulent motion ε can be expressed as

$$\varepsilon = C_D \frac{K^{3/2}}{\ell_{1D}} \quad (8)$$

Equation (8) has been used in the balance of K because of the small and isotropic nature of the dissipation. Here ℓ_{1D} and ℓ_{1v} are prescribed algebraically by Wolfstein,¹⁴ with

$$\ell_{1v} = C_D^{1/4} k_m y [1 - \exp(-0.016 R_T)] \quad (9)$$

to be used in the diffusivity and

$$\ell_{1D} = C_D^{1/4} k_m y [1 - \exp(-0.26 R_T)] \quad (10)$$

to be used in the dissipation. Here R_T is the local turbulent Reynolds number near a wall suggested by van Driest.⁹ The modified form used in the present work is

$$R_T = \frac{K^{1/2} y}{v} \quad (11)$$

and the maximum value of either ℓ_{1v} or ℓ_{1D} is replaced by

$$\ell_{1, \max} = C_D^{5/4} \delta \quad (12a)$$

for the cooled side, and by

$$\ell_{1, \max} = C_D^{5/4} (b - \delta) \quad (12b)$$

for the heated side.

The mixing-length constant k_m , devised for forced and mixed convection at low Reynolds numbers by Nakajima et al.,⁸ is similar to that proposed by Cebeci.¹⁵

$$k_m = 0.4[(0.974 - (20.77/\delta^+ - 5.48))] \quad (13)$$

In the region near the heated wall, i.e., $\delta < y < b$, y and δ^+ are replaced by $b - y$ and $(b^+ - \delta^+)z = (b_H^+ - \delta_H^+)z$ for the preceding equations where z is the correction factor to normalize the variable by means of the respective wall parameters of the cooled wall.

The boundary conditions for Eq. (1), (2), and (5) are as follows:

$$u = 0, \tau_w = -\mu \frac{du}{dy}, \quad T = T_c \text{ and } K = 0 \quad \text{at } y = 0 \quad (14a)$$

$$u = 0, \quad T = T_H \text{ and } K = 0 \quad \text{at } y = b \quad (14b)$$

By introducing the wall parameters at the cooled wall, Eqs. (1), (2), and (5) are normalized as

$$\frac{d}{dy^+} \left[(1 + v_T^+) \frac{du^+}{dy^+} \right] - \frac{dp^+}{dx^+} + G^+ \theta = 0 \quad (15)$$

$$\frac{d}{dy^+} \left[\left(\frac{1}{Pr} + \frac{v_T^+}{\sigma_T} \right) \frac{d\theta}{dy^+} \right] = 0 \quad (16)$$

$$\begin{aligned} \frac{d}{dy^+} \left[(1 + v_T^+) \frac{dK^+}{dy^+} \right] + v_T^+ \left(\frac{du^+}{dy^+} \right)^2 + \frac{v_T^+}{\sigma_T} \frac{d\theta}{dy^+} G^+ \\ - C_D \frac{v_T^+ K^+}{\ell_{1v}^+ \ell_{1D}^+} = 0 \end{aligned} \quad (17)$$

where

$$v_T^+ = \ell_{1v}^+ (K^+)^{1/2} \quad (18)$$

$$R_T^+ = (K^+)^{1/2} y^+ \quad (19)$$

$$\ell_{1v}^+ = C_D^{1/4} k_m y^+ [1 - \exp(-0.016 R_T^+)] \quad (20)$$

$$\ell_{1D}^+ = C_D^{1/4} k_m y^+ [1 - \exp(-0.26 R_T^+)] \quad (21)$$

The boundary conditions become

$$u^+ = 0, \quad \frac{du^+}{dy^+} = -1, \quad \theta = 0 \text{ and } K^+ = 0 \quad \text{at } y^+ = 0 \quad (22a)$$

$$u^+ = 0, \quad \theta = 1 \text{ and } K^+ = 0 \quad \text{at } y^+ = b^+ \quad (22b)$$

Numerical Method of Solution

To formulate a general solution by the finite-element method, the cubic element with a length ℓ and four nodes is used. The nodes are denoted by 1, 2, 3, and 4, and the nodal values by u_i^+ , θ_i , and K_i^+ , $i = 1, 2, 3, 4$. The shape functions, $N_1(\zeta)$, $N_2(\zeta)$, $N_3(\zeta)$, and $N_4(\zeta)$, can be defined as follows:

$$N_1(-1) = 1, \quad N_2(-1) = 0, \quad N_3(-1) = 0, \quad N_4(-1) = 0$$

$$N_1(-\frac{1}{3}) = 0, \quad N_2(-\frac{1}{3}) = 1, \quad N_3(-\frac{1}{3}) = 0, \quad N_4(-\frac{1}{3}) = 0$$

$$N_1(\frac{1}{3}) = 0, \quad N_2(\frac{1}{3}) = 0, \quad N_3(\frac{1}{3}) = 1, \quad N_4(\frac{1}{3}) = 0$$

$$N_1(1) = 0, \quad N_2(1) = 0, \quad N_3(1) = 0, \quad N_4(1) = 1$$

$$N_1(\zeta) + N_2(\zeta) + N_3(\zeta) + N_4(\zeta) = 1$$

Here ζ is the normalized local element coordinate, and the element is then defined by the range $-1 \leq \zeta \leq 1$.

Thus, the element equations become

$$\begin{aligned} u^+ &= \sum_{j=1}^4 N_j u_j^+ \\ \theta &= \sum_{j=1}^4 N_j \theta_j \\ K^+ &= \sum_{j=1}^4 N_j K_j^+ \end{aligned}$$

where

$$N_1(\zeta) = -\frac{9}{16}(\zeta + \frac{1}{3})(\zeta - \frac{1}{3})(\zeta - 1)$$

$$N_2(\zeta) = \frac{27}{16}(\zeta + 1)(\zeta - \frac{1}{3})(\zeta - 1)$$

$$N_3(\zeta) = -\frac{27}{16}(\zeta + 1)(\zeta + \frac{1}{3})(\zeta - 1)$$

$$N_4(\zeta) = \frac{9}{16}(\zeta + 1)(\zeta + \frac{1}{3})(\zeta - \frac{1}{3})$$

Employing the Galerkin weighted-residual approach, Eq. (15) becomes

$$\begin{aligned} \sum_1^{n^e} \int_{\ell} \left[\frac{dN_i}{dy^+} (1 + v_T^+) \frac{dN_j}{dy^+} u_j^+ + N_i \frac{dp^+}{dx^+} - N_i G^+ N_j \theta_j \right] dy^+ \\ - \left[N_i (1 + v_T^+) \frac{du^+}{dy^+} \right]_{s_1}^{s_2} = 0 \end{aligned} \quad (23)$$

where n^e = total number of elements (36 for the present work with larger concentrations in the regions near the walls and the maximum-velocity location; 32, 36, 40, and 44 elements were used, respectively, in the present calculations and it was found that 36 elements are sufficient to yield a grid-independent solution); $i, j = 1, 2, 3, 4$; s_1 and s_2 are boundaries of the element. Similarly, Eq. (16) becomes

$$\begin{aligned} \sum_1^{n^e} \int_{\ell} \left[\frac{dN_i}{dy^+} \left(\frac{1}{Pr} + \frac{v_T^+}{\sigma_T} \right) \frac{dN_j}{dy^+} \theta_j \right] dy^+ \\ - \left[N_i \left(\frac{1}{Pr} + \frac{v_T^+}{\sigma_T} \right) \frac{d\theta}{dy^+} \right]_{s_1}^{s_2} = 0 \end{aligned} \quad (24)$$

and Eq. (17) becomes

$$\sum_1^{ne} \int_{\ell} \left[\frac{dN_i}{dy^+} (1 + v_T^+) \frac{dN_j}{dy^+} K_j^+ - N_i v_T^+ \left(\frac{dN_k}{dy^+} u_k^+ \right)^2 - N_i \frac{v_T^+}{\sigma_T} \frac{dN_j}{dy^+} \theta_j G^+ + N_i C_D \frac{v_T^+ N_j}{\ell_{1v}^+ \ell_{1D}^+} K_j^+ \right] dy^+ - \left[N_i (1 + v_T^+) \frac{dK^+}{dy^+} \right]_{s_1}^{s_2} = 0 \quad (25)$$

where $i, j, k = 1, 2, 3, 4$.

Equations (23–25) are then combined into the form of assembled matrix equations

$$\tilde{A} \tilde{\lambda} = \tilde{B} \quad (26)$$

where the chosen form for $\tilde{\lambda}$ is

$$\lambda_j = \begin{bmatrix} u_j^+ \\ \theta_j \\ k_j^+ \end{bmatrix} \quad (27)$$

Each coefficient in the matrix \tilde{A} has the form

$$a_{ij} = \sum_1^{ne} \int_{\ell} \begin{bmatrix} c_{11} & c_{12} & c_{13} \\ c_{21} & c_{22} & c_{23} \\ c_{31} & c_{32} & c_{33} \end{bmatrix} dy^+ \quad (28)$$

where

$$\begin{aligned} c_{11} &= \frac{dN_i}{dy^+} (1 + v_T^+) \frac{dN_j}{dy^+}, & c_{12} &= -N_i G^+ N_j \\ c_{13} &= 0, & c_{21} &= 0, & c_{22} &= \frac{dN_i}{dy^+} \left(\frac{1}{Pr} + \frac{v_T^+}{\sigma_T} \right) \frac{dN_j}{dy^+} \\ c_{23} &= 0, & c_{31} &= 0, & c_{32} &= -N_i \frac{v_T^+}{i\sigma_T} \frac{dN_j}{dy^+} G^+ \\ c_{33} &= \frac{dN_i}{dy^+} (1 + v_T^+) \frac{dN_j}{dy^+} + N_i C_D \frac{v_T^+ N_j}{\ell_{1v}^+ \ell_{1D}^+} \end{aligned}$$

Each coefficient in the matrix \tilde{B} has the form

$$b_i = \sum_1^{ne} \int_{\ell} \begin{bmatrix} b_1 \\ b_2 \\ b_3 \end{bmatrix} dy^+ \quad (29)$$

where

$$\begin{aligned} b_1 &= -N_i \frac{dp^+}{dx^+}, & b_2 &= 0 \\ b_3 &= N_i v_T^+ \left(\frac{dN_k}{dy^+} u_k^+ \right)^2 \end{aligned}$$

There is a standard procedure to solve the preceding integrations: 1) normalizing the coordinate y^+ , and 2) using the Gaussian quadrature. In the present work, a four-Gaussian-integration sampling-point scheme is used. The initial values for iterative solution are to set K^+ as a constant with the value of about 3.0 in the equilibrium region. The convergence tolerance is 10^{-4} .

Reynolds number, Grashof number, Nusselt number, and friction factor are defined by Eqs. (30–35). Here δ is the distance from the cooled wall to the location at which the velocity has its maximum value. Nusselt number and friction factor are defined for both sides of the wall, i.e., the cooled and heated sides, which are bounded by the plane of $y = \delta$.

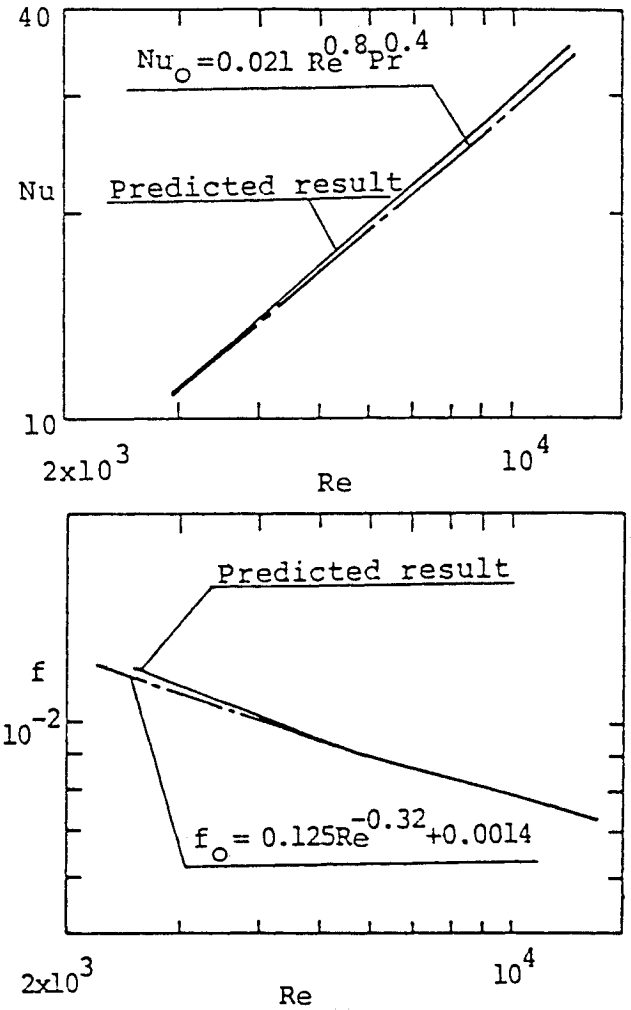


Fig. 2 Nusselt number and friction factor for forced convection.

Hence, these dimensionless groups are expressed as

$$Re = 2 \int_0^{b^+} u^+ dy^+ \quad (30)$$

$$Gr = 8b^+ G^+ \quad (31)$$

$$Nu_c = 4\delta^+ q^+ Pr / \langle \theta \rangle_c \quad (32)$$

$$Nu_H = 4(b^+ - \delta^+) q^+ Pr / (1 - \langle \theta \rangle_H) \quad (33)$$

$$f_c = 2 \left\{ \delta^+ / \int_0^{\delta^+} u^+ dy^+ \right\}^2 \quad (34)$$

$$f_H = 2 \left\{ z(b^+ - \delta^+) / \int_{\delta^+}^{b^+} u^+ dy^+ \right\}^2 \quad (35)$$

where

$$q^+ = \frac{1}{Pr} \frac{d\theta}{dy^+} \Big|_{y^+=0} \quad (36)$$

$$\langle \theta \rangle = \int_0^{b^+} \theta u^+ dy^+ / \int_0^{b^+} u^+ dy^+ \quad (37)$$

$$\langle \theta \rangle_c = \int_0^{\delta^+} \theta u^+ dy^+ / \int_0^{\delta^+} u^+ dy^+ \quad (38)$$

$$\langle \theta \rangle_H = \int_{\delta^+}^{b^+} \theta u^+ dy^+ / \int_{\delta^+}^{b^+} u^+ dy^+ \quad (39)$$

$$z = \sqrt{\frac{\tau_H}{\tau_c}} \quad (40)$$

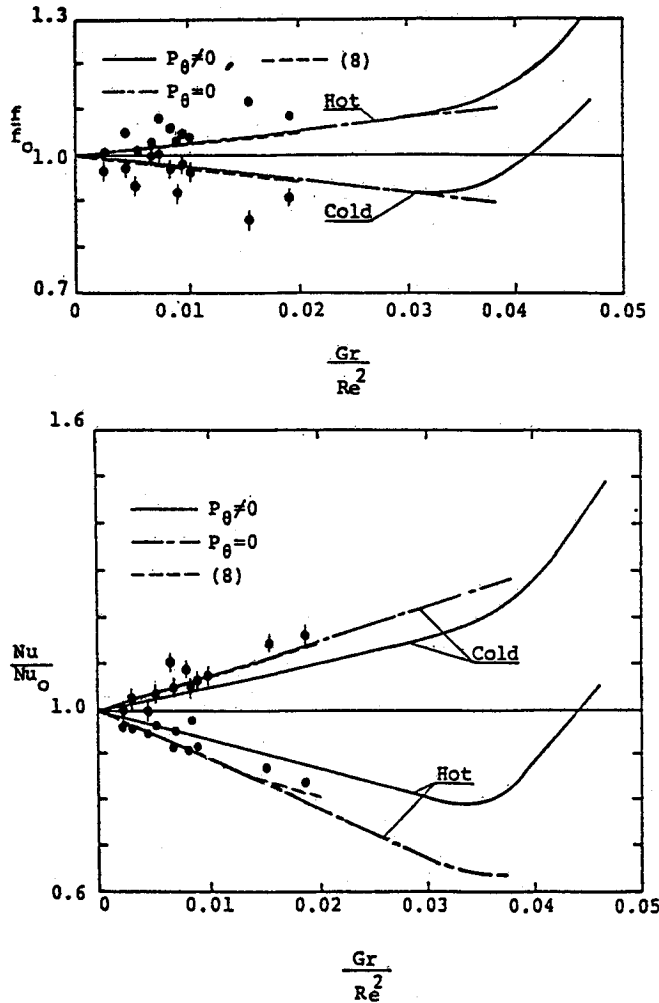


Fig. 3 Friction factor and Nusselt number for $Pr = 0.7$, $b^+ = 200$, and $Re = 5.885 \times 10^3$ for forced convection. (● experimental data by Nakajima et al.⁸).

Additionally, the Reynolds number Re is a variable and the differences among the Re are less than 3%; dp^+/dx^+ is also a variable given by

$$-\frac{dp^+}{dx^+} = \frac{1}{b^+} (|\tau_H^+| + 1) - G^+ \langle \theta \rangle \quad (41)$$

where

$$\tau_H^+ = \frac{\tau_H}{\tau_c}$$

and

$$-\frac{dp^+}{dx^+} = \frac{2}{b^+} \quad (42)$$

for forced convection.

Results and Discussion

To establish the relationships between flow, buoyancy influence, and friction factor or Nusselt number, pure forced convection must first be examined. The predicted results of friction factor and Nusselt number, shown in Figs. 2a and 2b for forced convection, are in good agreement with the familiar correlations, that is, the formula of McAdams¹⁶ for the heat transfer and that of Drew et al.¹⁷ for the friction factor

$$Nu_0 = 0.021 Re^{0.8} Pr^{0.4} \quad (43)$$

$$f_0 = 0.125 Re^{-0.32} + 0.0014 \quad (44)$$

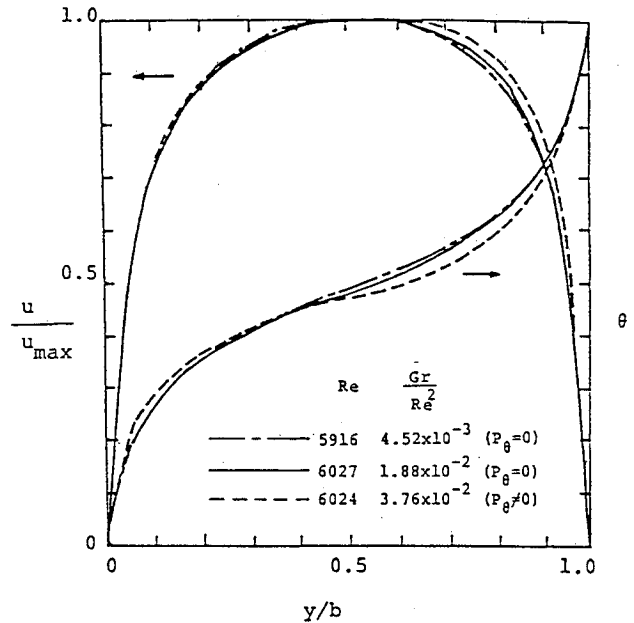


Fig. 4 Mean velocity and temperature profiles.

The predicted results of friction factor and Nusselt number for mixed flow of forced and natural convection are shown in Figs. 3a and 3b, respectively. For convenience, the parameter Gr/Re^2 is employed as an indicator for buoyancy force. The results are plotted in the form of Nu/Nu_0 and f/f_0 vs Gr/Re^2 and Pr held fixed ($Pr = 0.7$). On the heated side, the direction of the buoyancy force is the same as that of the flow. Accordingly, the stability of flow increases and the turbulent transfers of momentum and heat are inhibited. The buoyancy force causes an increase in the friction factor and a decrease in the Nusselt number. On the cooled side, the buoyancy force inhibits the flow of fluid. Accordingly, the instability increases, the friction factor decreases, and the Nusselt number increases. If the buoyancy production is not considered in the K equation when the buoyancy force is small, that is, $P_\theta = 0$, then the results are the same as those presented by Nakajima et al.⁸ However, no reasonable results can be obtained beyond $Gr/Re^2 = 0.038$, when the buoyancy production P_θ is assigned zero. Thus, the effect of buoyancy production is considered in the present investigation. In their study on pipe flow, Tanaka et al.¹⁰ found that the boundaries between forced and mixed convections and between mixed and natural convections can be defined, respectively, as $Nu/Nu_0 = 0.8$ and 1.0 . Because of the lack of reliable results for the channel flow case, their result is employed in the present study. From Fig. 3b, it is seen that the boundary between the forced and mixed convections is $Gr/Re^2 = 0.020$ and that between the mixed and natural convections is $Gr/Re^2 = 0.044$.

Figure 3b shows that the comparison between the experimental data as well as the numerical results of Nakajima et al.⁸ and the current results is satisfactory. Thus, the turbulent model used in the present work is valid and can predict the result in the ranges of mixed convection and natural convection. The model used by Nakajima et al.⁸ can only predict the result in the range of forced convection and cannot predict the effect of buoyancy force on turbulence kinetic energy. Accordingly, the current model is more effective than that used by Nakajima et al.⁸ It can also be seen in Fig. 3b that the variation of Nusselt number at the cooled side is similar to that of Tanaka et al.¹⁰

The distributions of the mean velocity and temperature for mixed convection are shown in Fig. 4. When buoyancy production is considered, the velocity distributions are steeper for both regions near the cooled and heated sides, especially in the region near the heated side. Furthermore, the dimensionless temperature distribution increases in the region near the

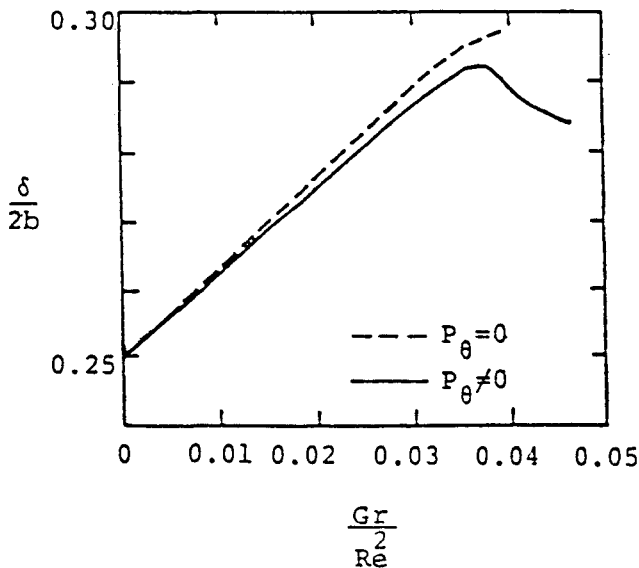


Fig. 5 Distance from cooled wall to maximum-velocity location.

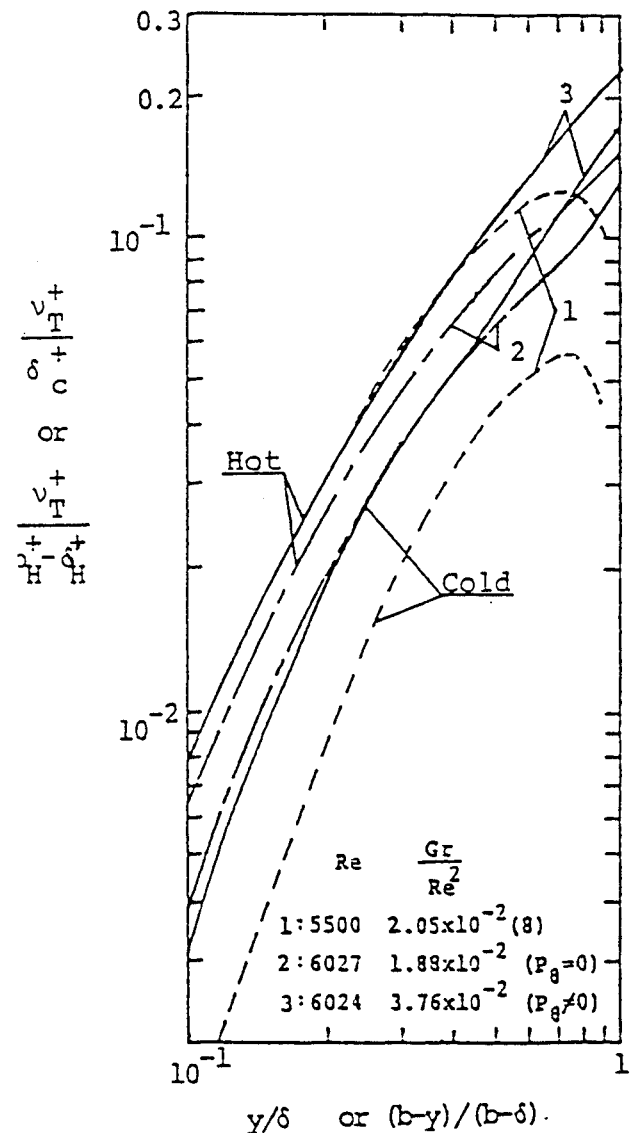


Fig. 6 Eddy diffusivities for momentum.

cooled side and decreases in the region near the heated side. Accordingly, it is flatter in the middle region and more symmetrical about the middle point.

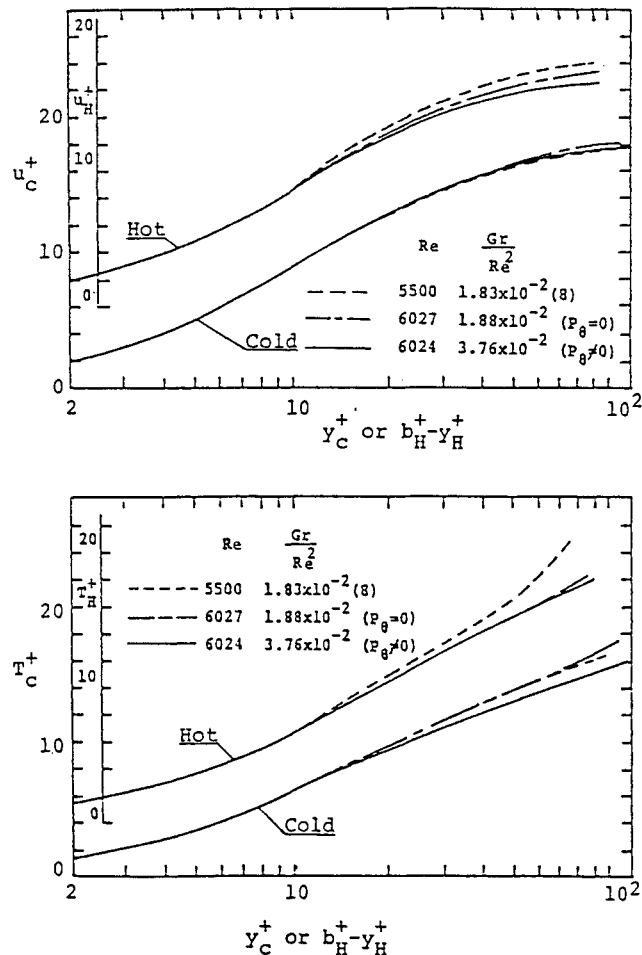


Fig. 7 Mean velocity and temperature profiles normalized with wall parameters.

The distance from the cooled wall to the location of the maximum velocity is shown in Fig. 5. It is seen from Fig. 5 that for the situation of $P_\theta = 0$, the location of maximum velocity gets closer to the heated wall because of the absence of intensification of turbulence by the buoyancy force.

The predicted eddy diffusivities for momentum transfer are plotted in Fig. 6. The results presented by Nakajima et al.⁸ are unreasonable, because there is no reason for ν_T to vanish at the point with zero velocity gradient. Equation (3) is used to modify the aforementioned inadequacy in one-equation models. It can be seen in Fig. 6 that eddy diffusivities increase in the region near the cooled wall and decrease in the region near the heated wall as Gr/Re^2 increases. However, in the fully turbulent region, i.e., $y/\delta > 0.2$, the buoyancy effect is significant.

The predicted distributions of velocity and temperature for mixed convection, normalized by respective wall parameters, are shown in Fig. 7. As before, the results obtained by Nakajima et al.⁸ are not reasonable in the region near the location of maximum velocity, because T_c^+ and T_H^+ should be flatter rather than steeper in this region, as shown in Fig. 7.

The distributions of turbulence kinetic energy in the regions near the walls and in the fully turbulent region are shown in Figs. 8a and 8b, respectively. The normalizations for the heated and cooled sides are done with respective wall parameters. It is shown in Fig. 8 that the turbulence kinetic energy increases in the region near the cooled wall and decreases in the region near the heated wall as Gr/Re^2 increases. The influence of buoyancy production is not significant in the wall regions. However, significant buoyancy effects exist in the fully turbulent region. The buoyancy force causes an increase in turbulence kinetic energy and eddy diffusivities. The phenomena shown in Figs. 4–6 are thus confirmed.

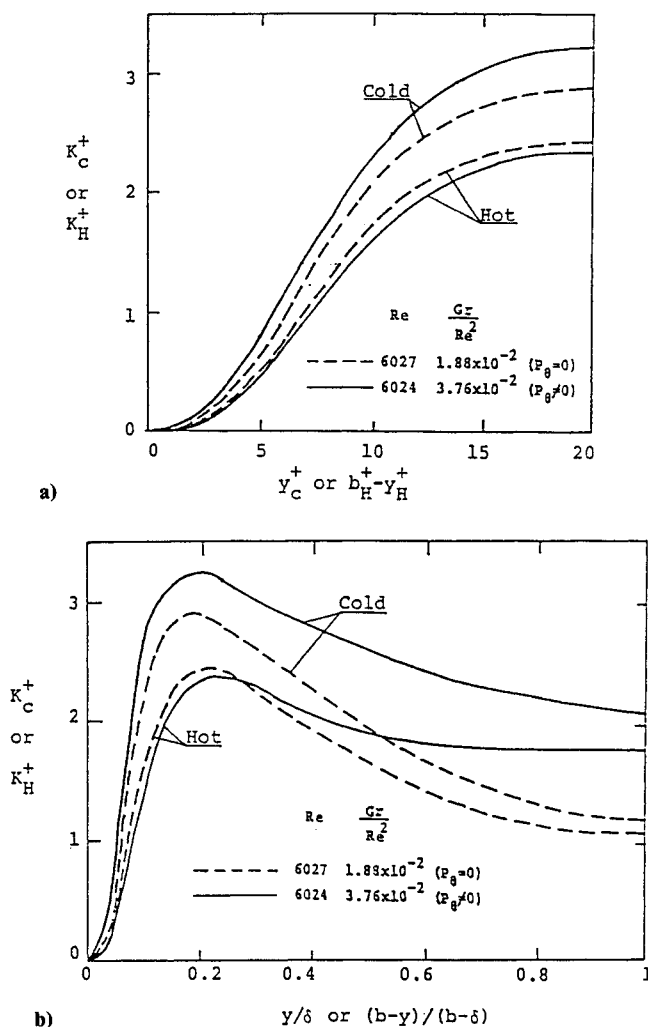


Fig. 8 Normalized turbulence kinetic energy a) in the wall regions, and b) in the fully turbulent region.

Conclusions

In the present work, the influence of buoyancy production in turbulent combined forced and natural convection is studied. One-equation models with and without buoyancy production are considered in fully developed turbulent transport between two vertical parallel plates within isothermal walls at different temperatures.

In opposing flow, in which the buoyancy force is exerted in a direction opposite to the flow, the Nusselt number with the inclusion of buoyancy production is lower than that without considering buoyancy production. In aiding flow, in which the buoyancy force acts in the flow direction, the variations of Nusselt number are the reverse of the opposing flow. This indicates that buoyancy production reduces the difference in heat transfer between opposing and aiding flows. In the forced convection region of aiding flow, that is, $Nu > 0.8Nu_0$, the neglect of buoyancy production is acceptable according to the experiment by Nakajima et al.⁸ But in the mixed convection region of aiding flow, that is, $0.8Nu_0 < Nu < Nu_0$, the viscous production alone cannot represent the turbulence intensity of

the flowfield. Thus, buoyancy production must be considered in order to accurately predict the flowfield and the results of natural convection in the region $Nu > Nu_0$ of aiding flow. In addition, the friction factor is affected by buoyancy production in mixed and natural flows.

All physical phenomena, including velocity profiles, distributions of temperature and turbulence kinetic energy, eddy diffusivities for momentum and for heat, are not influenced significantly by the buoyancy production in the regions near walls. However, for the fully turbulent region, the influence of buoyancy production is significant and cannot be neglected, especially in mixed and natural convection.

References

- 1Brown, C. K. and Gauvin, W. H., "Combined Free and Forced Convection," *The Canadian Journal of Chemical Engineering*, Vol. 43, 1965, pp. 306-318.
- 2Brown, C. K. and Gauvin, W. H., "Temperature Profiles and Fluctuations in Combined Free- and Forced-Convection Flows," *Chemical Engineering Science*, Vol. 21, 1966, pp. 961-970.
- 3Buhr, H. O., Carr, A. D., and Balzhiser, R. E., "Temperature Profiles in Liquid Metals and the Effect of Superimposed Free Convection in Turbulent Flow," *International Journal of Heat and Mass Transfer*, Vol. 11, 1968, pp. 641-653.
- 4Hall, W. B. and Price, P. H., "Mixed Forced and Free Convection from a Vertical Heated Plate to Air," *4th International Heat Transfer Conference*, Vol. 4, NC 3.3, 1970, pp. 1-10.
- 5Kenning, D. B. R., Shock, R. A. W., and Poon, J. Y. M., "Local Reductions in Heat Transfer Due to Buoyancy Effects in Upward Turbulent Flow," *5th International Heat Transfer Conference*, Vol. 3, NC 4.3, 1974, pp. 139-143.
- 6Tanaka, H., Tsuge, A., Hirata M., and Nishiwaki, N., "Effects of Buoyancy and of Acceleration Owing to Thermal Expansion on Forced Turbulent Convection in Vertical Circular Tubes—Criteria of the Effects, Velocity, and Temperature Profiles, and Reverse Transition from Turbulent to Laminar Flow," *International Journal of Heat and Mass Transfer*, Vol. 16, June 1973, pp. 1267-1288.
- 7Khosla, J., Hoffman, T. W., and Pollock, K. G., "Combined Forced and Natural Convective Heat Transfer to Air in a Vertical Tube," *5th International Heat Transfer Conference*, Vol. 3, NC 4.4, 1974, pp. 144-148.
- 8Nakajima, M., Fukui, K., Veda, H., and Mizushima, T., "Buoyancy Effects on Turbulent Transport in Combined Free and Forced Convection Between Vertical Parallel Plates," *International Journal of Heat and Mass Transfer*, Vol. 23, Oct. 1980, pp. 1325-1336.
- 9van Driest, E. R., "On Turbulent Flow Near a Wall," *Journal of Aerodynamics Science*, Vol. 23, 1956, pp. 1007-1011.
- 10Tanaka, H., Maruyama, S., and Hatano, S., "Combined Forced and Natural Convection Heat Transfer for Upward Flow in a Uniformly Heated, Vertical Pipe," *International Journal of Heat and Mass Transfer*, Vol. 30, Jan. 1987, pp. 165-174.
- 11Townsend, A. A., *The Structure of Turbulent Shear Flow*, 2nd ed., Cambridge Univ. Press, New York, 1976.
- 12Kader, B. A. and Yaglom, A. M., "Heat and Mass Transfer Laws for Fully Turbulent Flows," *International Journal of Heat and Mass Transfer*, Vol. 15, 1972, pp. 2329-2351.
- 13Ng, K. H. and Spalding, D. B., "Turbulence Model for Boundary Layers near Walls," *Physics of Fluids*, Vol. 15, Jan. 1972, pp. 20-30.
- 14Arpaci, V. S. and Larson, P. S., *Convection Heat Transfer*, 1st ed., Prentice-Hall International, London, 1984, Chap. 10.
- 15Cebeci, T., "A Model for Eddy Conductivity and Turbulent Prandtl Number," *Journal of Heat Transfer, Transactions of ASME*, Vol. 95C, May 1973, pp. 227-234.
- 16McAdams, W. H., *Heat Transmission*, 3rd ed., McGraw-Hill, New York, 1954.
- 17Drew, T. B., Koo, E. C., and McAdams, W. H., "The Friction Factor for Clean Round Tubes," *Transactions of the American Institute of Chemical Engineers*, Vol. 28, 1932, pp. 56-72.